

## DYNAMIC LOADING TEST ON RC FRAME RETROFITTED BY OUTER CES FRAME

Takashi TAGUCHI<sup>1</sup>, Hiroshi KURAMOTO<sup>2</sup>, Tomoya MATSUI<sup>3</sup> and Takashi KAMIYA<sup>4</sup>

<sup>1</sup>Head Research Engineer, Tech. Res. Inst. for Earthquake Eng., Yahagi Const. Co., Ltd., Nagoya, Japan

<sup>2</sup>Professor, Div. of Global Architecture, Graduate School of Eng, Osaka Univ., Suita, Japan

<sup>3</sup>Assistant Professor, Dept. of Architecture & Civil Engineering, Toyohashi Univ. Tech., Toyohashi, Japan

<sup>4</sup>Sub Manager, Tech. Res. Inst. for Earthquake Eng., Yahagi Const. Co., Ltd., Nagoya, Japan

Email: t-taguchi@yahagi.co.jp, kuramoto@arch.eng.osaka-u.ac.jp, matsui@tutrp.tut.ac.jp,  
t-kamiya@yahagi.co.jp

### ABSTRACT :

The authors have proposed a seismic retrofitting method by attaching outer CES frames consisting of only steel and fiber reinforced concrete to an existing RC building. This method has more advantage compared with previous proposed other seismic retrofitting methods that is not necessary to install the braces because CES frames in themselves have excellent seismic performance. The purpose of this study is to investigate the seismic performance of RC frames retrofitted with CES frames, particularly to examine the behavior of unified sections of the existing RC and the strengthening CES. The dynamic load testing was carried out on four frame specimens, one RC frame and three retrofitted RC frames, with the experimental parameter of the amount of anchors used to connect the CES members to the RC members. This paper outlines the experimental program. The test results showed that the seismic retrofitting method by attaching the CES member to RC member improved the seismic performance of the frames. It was observed that there is almost no gap at the connection between CES member and RC member until large deformation. In addition, the ultimate strength of the retrofitted frame from the experimental results showed a good agreement with the calculated ultimate strength.

**KEYWORDS:** Concrete encased steel, Fiber reinforced concrete, External seismic retrofit, Retrofitted RC frame, Dynamic loading test

### 1. INTRODUCTION

Concrete encased steel (CES) structures are composite structural systems consisting of steel and concrete. Previous Paper has shown that CES structures using fiber reinforced concrete (FRC) show hysteresis characteristics and damage reduction effects more than the equal to that of steel reinforced concrete (SRC) structures [1,2].

The authors have proposed to apply CES structures to the seismic retrofitting of an existing RC building [3]. This method has more advantage compared with previous proposed other seismic retrofitting method that is not necessary to install braces because CES frames had been proved to have excellent hysteresis behavior. Therefore, since this method enables to construct the retrofitting without closing the openings and changing the planning in existing RC buildings, it suits to be used for the retrofitting of relatively large-scale buildings such as apartment houses, office buildings and commercial buildings in shown Fig. 1. Previous research, this method has confirmed that an excellent seismic retrofitting effect is achieved by applying an externally CES retrofit to RC columns and RC frames [3].

The purpose of this study is to investigate the seismic performance of RC frame retrofitted by CES frames, particularly to examine the behavior of unified sections by existing RC and strengthening CES. The dynamic loading test is carried out on four frame specimens, one RC frame and three RC retrofitted frames, with the experimental parameter of the amount of anchor used to the boundary of the CES member to the RC member. This paper outlines the experimental program and the test results.

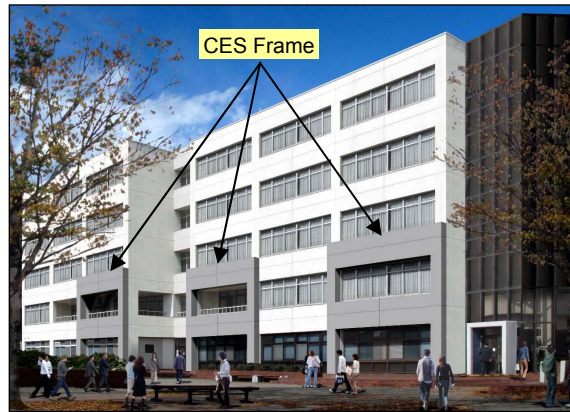


Figure 1 Concept of the RC frame externally retrofitted by CES frame

## 2. EXPERIMENTAL PROGRAM

### 2.1. Specimens

The specimens used for the experiment were four frames, one existing RC frame (Specimen FP3) and three existing RC frames externally retrofitted by CES frame (Specimens FC31, FC32 and FC33). The experimental parameter of the retrofitted specimens was the amount of anchors used to connect the CES member to the RC member. The amount of number to be installed in each member was calculated as follows. The amount of anchor to the specimen FC31 was carried out in accordance with reference [4]. Estimates were made to allow transmission of both the ultimate shear yield strength (horizontal force) of CES column members in the connection of the beams, and the ultimate shear yield strength (vertical force) of the CES beam in the connection of the columns respectively. In specimens FC32 and FC33 the amount of anchors was made, respectively, 0.7 times and 0.5 times the amount used in specimen FC31. The retrofitted specimen is shown in Table 1 and Fig. 2.

The specimens were approximately 1/2 scale of actual sizes. The columns' inside height measurement was  $h_o=1,100\text{mm}$  (shear span ratio:  $M/QD=1.83$ ). In the column cross-section, the existing member was  $300\times 300\text{mm}$  and the retrofitting member was  $150\times 300\text{mm}$  in dimension. The inside measurement of the beams were  $l=2,700\text{mm}$  (shear span ratio to retrofitting member:  $M/QD=3.38$ ). In the beams cross-section, the existing member was  $300\times 710\text{mm}$  and the retrofitting member was  $150\times 400\text{mm}$  in dimension. The built-in steel of the retrofitting member of the columns and beams, size H-250 $\times$ 100 $\times$ 9 $\times$ 9 and H-300 $\times$ 100 $\times$ 9 $\times$ 9 were used.

Tables 2 and 3 show the material testing results of the reinforcement and the steel used by the experiment. Table 4 shows the material testing results for both the normal concrete used in the existing members and the FRC used for the retrofitting members. The fiber used for the FRC was polyvinyl alcohol fiber which is 0.66mm in the diameter and 30mm in length, and the volume mixing rate used was 1.0%.

Table 1 Outline of specimen

Specimen		FP3		FC31		FC32		FC33	
Member		Column	Beam	Column	Beam	Column	Beam	Column	Beam
Existing Member	Concrete	Normal Concrete							
	$b(\text{mm})\times D(\text{mm})$	300 $\times$ 300	300 $\times$ 710	300 $\times$ 300	300 $\times$ 710	300 $\times$ 300	300 $\times$ 710	300 $\times$ 300	300 $\times$ 710
	Main Reinforcement	10-D16 SD295	12-D25 SD345	10-D16 SD295	12-D25 SD345	10-D16 SD295	12-D25 SD345	10-D16 SD295	12-D25 SD345
	Hoop	2-D6@150 SD295	3-D13@85 SD345	2-D6@150 SD295	3-D13@85 SD345	2-D6@150 SD295	3-D13@85 SD345	2-D6@150 SD295	3-D13@85 SD345
Retrofitting Member	Concrete	Fiber Reinforced Concrete							
	$b(\text{mm})\times D(\text{mm})$	-	-	150 $\times$ 300	150 $\times$ 400	150 $\times$ 300	150 $\times$ 400	150 $\times$ 300	150 $\times$ 400
	Steel	-	-	H-250 $\times$ 100	H-300 $\times$ 100	H-250 $\times$ 100	H-300 $\times$ 100	H-250 $\times$ 100	H-300 $\times$ 100
Amount of Anchor		-	-	10	32	8	22	6	16

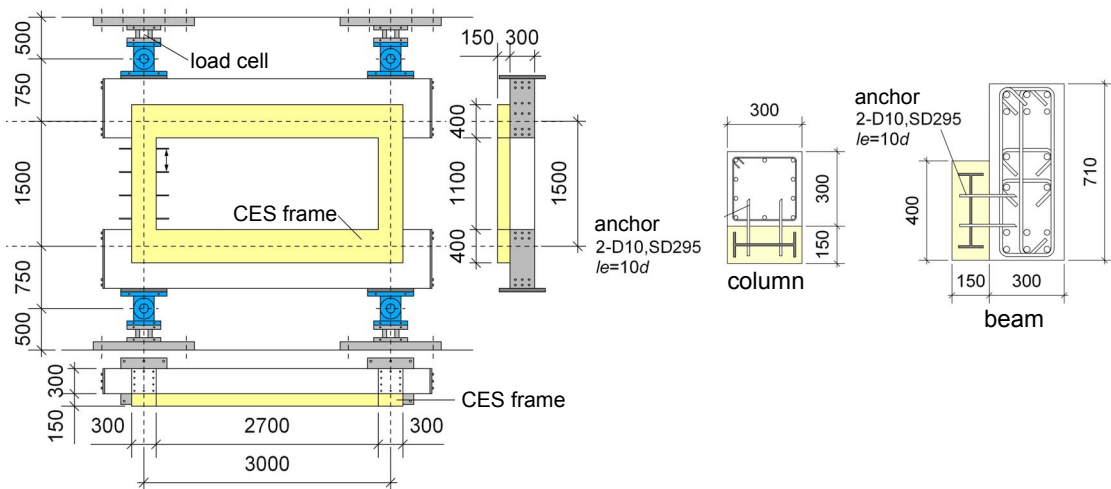


Figure 2 Test specimen

Table 2 Material properties of rebar

Reinforcing Bar	Steel Material	Yielding Stress (N/mm <sup>2</sup> )	Tension Strength (N/mm <sup>2</sup> )	Young's Modulus (×10 <sup>3</sup> N/mm <sup>2</sup> )	Member
D6	SD295	352.5	524.9	184.3	Column Hoop
D10	SD295	333.6	469.4	181.9	Anchor
D16	SD295	346.4	516.9	185.5	Main Reinforcement

Table 3 Material properties of plate

Plate	Steel Material	Yielding Stress (N/mm <sup>2</sup> )	Tension Strength (N/mm <sup>2</sup> )	Young's Modulus (×10 <sup>3</sup> N/mm <sup>2</sup> )	Member
PL-9	SN400B	290.1	439.5	209.3	Column, Beam
PL-16	SN490C	364.7	537.2	207.8	Beam-Column Connection

Table 4 Material properties of concrete

Specimen	Type	Compressive Strength (N/mm <sup>2</sup> )	Young's Modulus (×10 <sup>3</sup> N/mm <sup>2</sup> )
FP3	Normal Concrete	14.9	20.5
FC31	Normal Concrete	14.6	20.6
	Fiber Reinforced Concrete	29.9	21.8
FC32	Normal Concrete	15.0	20.9
	Fiber Reinforced Concrete	28.0	22.7
FC33	Normal Concrete	14.6	20.9
	Fiber Reinforced Concrete	26.8	22.5

### 2.2. Dynamic Loading Test

The dynamic loading apparatus used in the experiment is shown in Fig. 3. In the experiment, using two static vertical actuators, the columns were loaded with a constant compression axial of 270kN (an equivalent axial force ratio of 0.2 on existing RC columns) for each column. Then, a sinusoidal wave of a dynamic horizontal actuator was excited by displacement control. The loading programs were controlled by drift angle  $R$ , which was given by the height between the up and down beam-column connections. Waves were applied at  $R=0.002, 0.0033, 0.005, 0.01, 0.015, 0.02, 0.025, 0.03, \text{ and } 0.04$  radians; five waves for each cycle. The excitation frequency was set at a base of 1.5Hz. However, the frequency was reduced to 1.0Hz and 0.5Hz in consideration of the performance limitations of the actuator (maximum velocity: 50cm/sec) at times of large deformation.

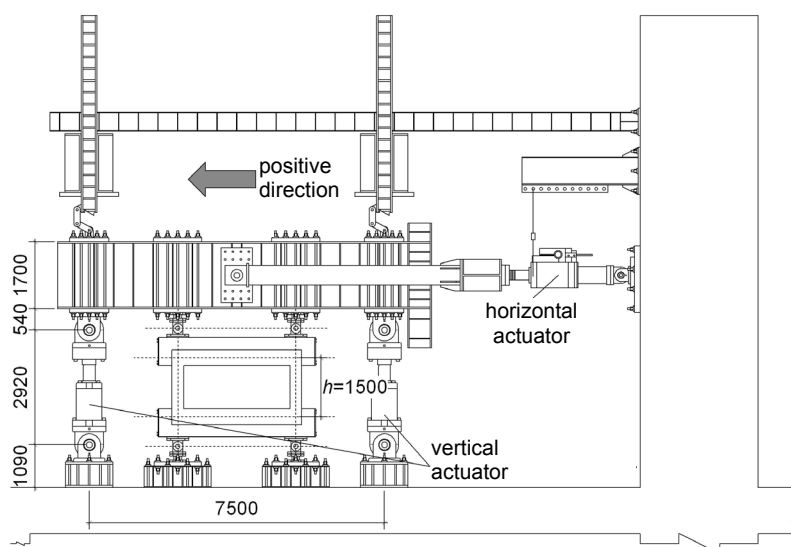


Figure 3 Dynamic loading apparatus

### 3. EXPERIMENTAL RESULTS

#### 3.1. Crack and Failure Modes

The crack modes for  $R=0.01$  radians on the front and rear surfaces for each specimen are shown in Fig. 4, and the final failure modes are shown in Fig. 5. In the retrofitted specimens, the front surface is the CES retrofitting side, and the rear surface is an existing RC side. The final failure modes are those at the time the experiment ended for each specimen. The failure modes are, for specimen FP3, the condition at the end of a load cycle of  $R=0.015$  radians, and, for each retrofitted specimen, the condition at the end of a load cycle of  $R=0.04$  radians.

In the case of non-retrofitted specimen FP3 a shearing crack occurred in the column at an  $R=0.005$  radians, and at an  $R=0.01$  radians the shearing crack of the column spread over the wide area. After this, at an  $R=0.015$  radians, the concrete of the front and rear surfaces of the specimen broke away.

In the case of CES retrofitted specimen FC31, multiple bend cracks appeared across the entire beam of the retrofitting member at an  $R=0.002$  radians, and cracks were confirmed along the flange of the beam and the beam-column connection at an  $R=0.0033$  radians. When  $R=0.005$  radians, the bend cracks occurred in the column of the retrofitting member. At an  $R=0.01$  radians, the shearing cracks occurred in the column of the existing member, and cracks were confirmed in the boundary of the retrofitting member and existing member of the beam-column connection. In the retrofitting member, at an  $R=0.015$  and  $0.02$  radians, beam's bend cracks and crack along the flange continued to progress. In the existing member, the shearing cracks of the column progressed over a wider area. At an  $R=0.025$  radian and beyond, in the column in the existing member, along with the continued development of the shear cracks, the concrete of the rear surface fell away. On the other hand, in the case of the retrofitting members, even in their final fracture condition, no fell away of concrete could be confirmed. Moreover, while the occurrence of cracks was perceived in several places in the boundary between the retrofitting and existing members of the beam, neither slippage nor opening could be perceived by visual inspection.

The crack and the failure modes of retrofitted specimens FC32 and FC33, in comparison with specimen F31, showed, at an initial cycle such as  $R=0.002$  radians and  $R=0.0033$  radians, some slightly different properties. However, at an  $R=0.005$  radians and beyond they showed the same tendencies.

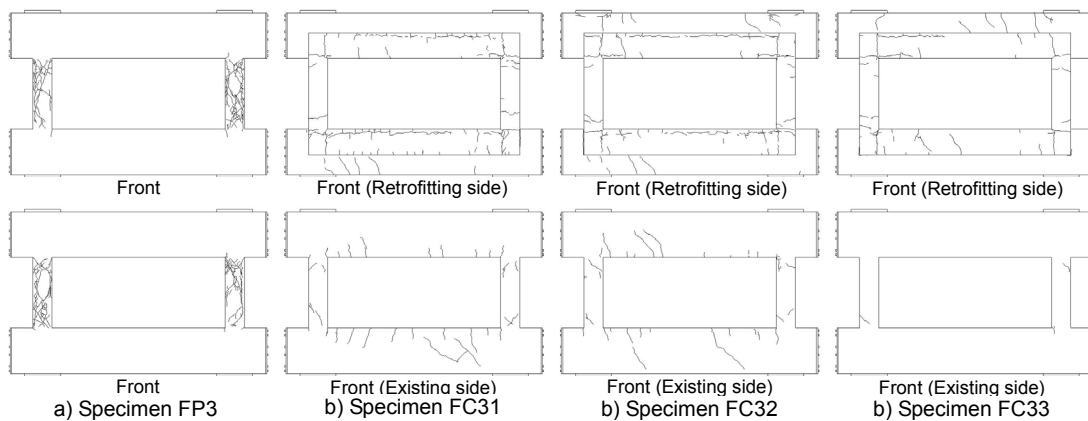


Figure 4 Crack conditions ( $R=0.01$  radians)

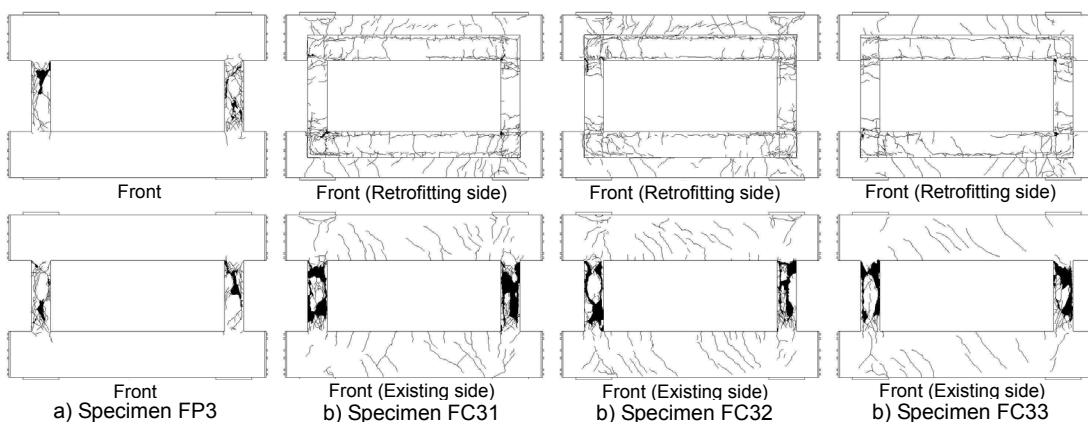


Figure 5 Final failure modes

### 3.2. Hysteresis Characteristics

The experimental results are listed in Table 5, and the shear force versus horizontal deformation relationships are shown in Fig. 6. In these, the shear force uses the values measured with the load cell installed on the specimen. Moreover, in the figure, the maximum strength point and the first yield points measured by strain gauge attached to the specimen are shown. The straight line, the dotted line, the dashed-dotted line in the hysteresis curve shows the histories of excitation frequencies 1.5, 1.0 and 0.5Hz respectively. Also, the ultimate strength value of calculated are shown by dashed-dotted straight lines.

In specimen FP3, on the positive load side, the hoop of the column yielded to an  $R=0.006$ , and the shear force rapidly decreased at an  $R=0.008$  radians after having recorded a maximum strength point 392.6kN. For the CES retrofitted specimen FC31, the column steel flange yielded at  $R=0.006$  radians, main reinforcement of the column yielded at  $R=0.007$  radians, the beam steel flange yielded at  $R=0.008$  radians, and the hoop of the column yielded at  $R=0.009$  radians. The recorded maximum strength point was 856.0kN at  $R=0.013$  radians. There was no rapid the shear force decrease as in specimen FP3, and at the final drift angle a high shear force, 639.2kN was sustained. However, a slight decrease in shear force with an accompanying hysteresis loop disturbance on the positive load side at a cycle of  $R=0.04$  radians. The various members of the specimen FC32 yielded at a drift angle almost the same as that of test specimen FC31, and recorded maximum strength point 886.9kN at an  $R=0.013$  radians. The subsequent shear force decrease was gradual, 628.4kN was recorded at the final drift angle, and it showed spindle type stable behavior, not becoming disordered, right through to its final drift angle. For the specimen FC33, the column steel flange yielded at an  $R=0.006$  radians, the beam steel flange at  $R=0.007$  radians, main reinforcement of the column at  $R=0.008$  radians, and hoop of the column at  $R=0.009$  radians. It recorded maximum strength point of 888.3kN at  $R=0.0133$  radians. The subsequent shear force decrease was gradually, 620.7kN was recorded at the final drift angle. This specimen showed the same stable spindle type behavior as specimen FC32.

While each of the retrofitted the specimens showed almost the same hysteresis properties, in the case of specimen FC31, its slight degradation in shear force on the positive load side of the cycle of  $R=0.04$  radians was conspicuous. It has been surmised that the reason for this was that specimen FC31 had the largest amount of anchors, and at the time of large deformation the anchors placed in the column promoted damage of the existing member of the specimen.

Table 5 List of experimental results

Specimen	Direction	Experimental Results										Calculate Ultimate Strength Value	Ratio to Results
		Yield Point								Maximum Strength Point			
		Main Reinforcement		Hoop		Column Flange		Beam Flange		$E R_{max}$ (rad.)	$E P_{max}$ (kN)	$A P_{max}$ (kN)	$E P_{max} / A P_{max}$
		$R_y$ (rad.)	$P_y$ (kN)	$R_y$ (rad.)	$P_y$ (kN)	$R_y$ (rad.)	$P_y$ (kN)	$R_y$ (rad.)	$P_y$ (kN)				
FP3	Positive	0.007	370.1	0.006	351.1					0.008	392.6	235.8	1.66
	Negative	-0.008	-177.3	-	-					-0.004	-285.7		1.21
FC31	Positive	0.007	713.4	0.009	780.4	0.006	658.0	0.008	751.3	0.013	856.0	722.8	1.18
	Negative	-0.007	-758.8	-	-	-0.005	-646.2	-0.006	-702.1	-0.008	-788.3		1.09
FC32	Positive	0.007	691.3	0.009	685.5	0.006	623.8	0.008	732.4	0.013	886.9	721.7	1.23
	Negative	-0.007	-750.9	-	-	-0.004	-617.7	-0.007	-782.0	-0.011	-899.5		1.25
FC33	Positive	0.008	746.2	0.009	768.2	0.006	664.4	0.007	710.0	0.013	888.3	718.2	1.24
	Negative	-0.007	-746.5	-	-	-0.004	-592.9	-0.006	-664.9	-0.011	-850.8		1.18

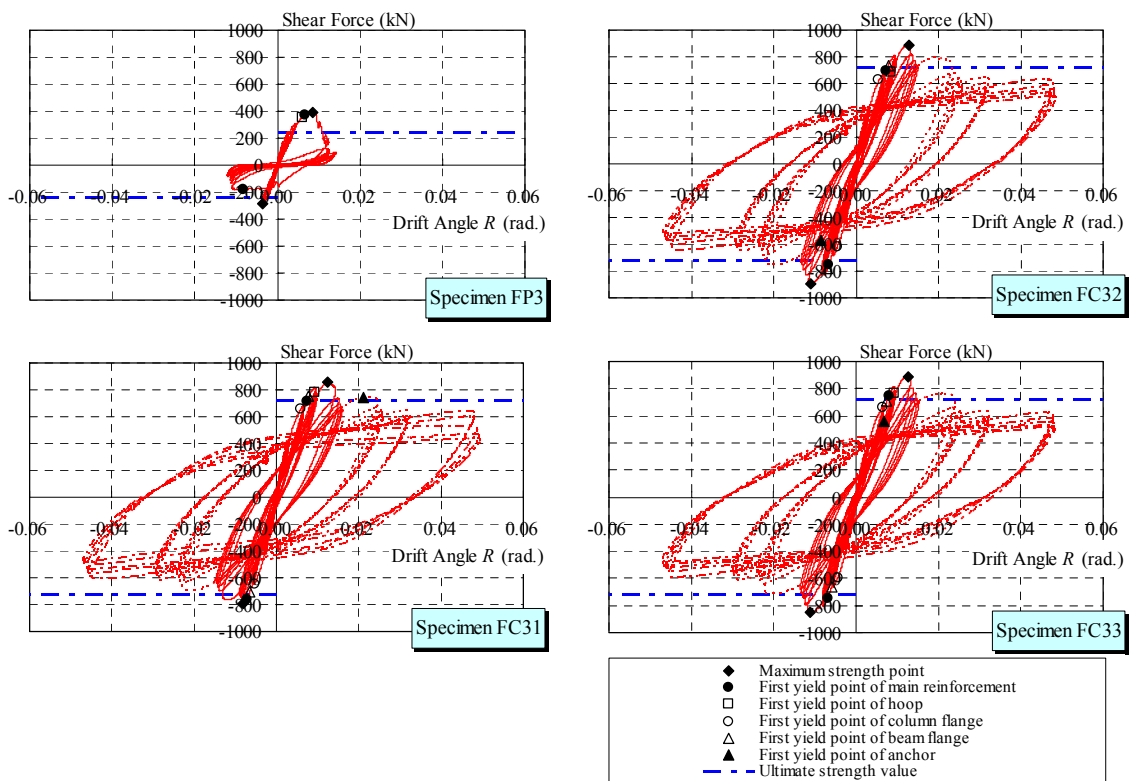


Figure 6 Shear force – horizontal deformation relationships

### 3.3. Shift of Existing and Retrofitting members

The shift of in-plane shearing (X and Y direction) and out-plane shearing for the beam-column connection, and for the boundary of columns and beams existing members and retrofitting members, are shown in Figs. 7, 8 and 9. Moreover, the definition in direction of each shearing and the measurement locations of the members are shown in Fig. 10. The measurement values shown are the maximum value at each load cycle.

In the beam-column connection shearing hardly occurred up to an  $R=0.005$  radians. Over an  $R=0.01$  radians shift was generated in out-plane and in both X and Y directions of the in-plane. At an  $R=0.03$  radians, the shift

of up to approximately 3mm was caused in the Y direction of the in-plane. In the columns, almost no shift occurred up to an  $R=0.01$  radians, and the shift was generated rapidly over an  $R=0.015$  radians. However, in the beams, even up to the final deformation angle, no large scale shift was generated, the largest being about 0.6mm. Moreover, no significant difference could be ascertained in the amount of the shift in each of the retrofitted specimens.

In this experiment, the adopted loading method exerted a shear force along the member axis in the existing RC frame. Therefore, the eccentric moment is generated in the retrofitting CES frame. It is thought that the early shift of the beam-column connection was generated. Moreover, while large scale shifts of the column was confirmed at over  $R=0.015$  radians, it has been considered that it is because the existing column was greatly damaged in section 3.1.

#### 4. CONCLUSIONS

In order to examine the influence that the amount of anchors installed in the boundary of existing member and retrofitting member exerts on the stiffening effect, as fundamental research into seismic reinforcement using CES structures, a dynamic loading test of RC frames with externally CES retrofit was conducted, with the amount of anchors set as a parameter. The findings obtained in this research are summarized below.

- 1) Three cases were compared, a case with the amount of anchors following previous design conventions (FC31), and cases with 0.7 times and 0.5 times the amount used in specimen FC31 (FC32 and FC33). The results of this comparison showed that there were no large differences perceived in the hysteresis characteristics, in the failure modes, in the shift of the retrofitting members and the existing members.
- 2) RC frames externally retrofitted by CES frames, regardless of the amount of anchors, each showed stable and excellent hysteresis properties in their energy absorption ability. At the time of large deformation, however, the damage to existing RC members is promoted by the attachment of a large amount of anchors, there is a possibility of promoting yield strength degradation.
- 3) Shift deformation in the boundary of the existing RC members and the CES retrofitting members is hardly perceivable until the maximum strength ( $R=0.015$  radians). Moreover, while some shearing deformations grow larger when above maximum strength, this originates in the progress of breakage in the existing RC members.
- 4) As for the ultimate strength of the existing RC frames externally retrofitted by CES frames, it can be evaluated by simple cumulative addition of the flexural strength calculation value of the CES member and the existing RC members' strength calculation value (shearing strength or bending strength).

#### REFERENCES

- [1] Adachi, T., Kuramoto H., Oike, K. and Kawasaki K. (2002). Experimental study on elasto-plastic behavior of composite CES columns using FRC. *Summaries of Technical Papers of Annual Meeting*, Architectural Institute of Japan, Vol.C-1, 1025-1026. (in Japanese)
- [2] Sasaki, T., Taguchi, T., Kawamoto, T., Nagata, S., Matsui, T. and Kuramoto, H. (2006). Experimental studies on structural characteristics of CES-columns (Part 1 and 2). *Summaries of Technical Papers of Annual Meeting*, Architectural Institute of Japan, Vol.C-1, 1067-1070. (in Japanese)
- [3] Suzuki, M., Sato, M., Hirose, T., Haga, R., Fukatsu, N., Taguchi, T., Kamiya, T., Matsui, T. and Kuramoto, H. (2007). Development of CES outer frame for retrofitting (Part 1, 2, 3, 4 and 5). *Summaries of Technical Papers of Annual Meeting*, Architectural Institute of Japan, Vol.C-1, 1277-1286. (in Japanese)
- [4] The Japan Building Disaster Prevention Association (2001). *Seismic Evaluation and Retrofit* (in Japanese)

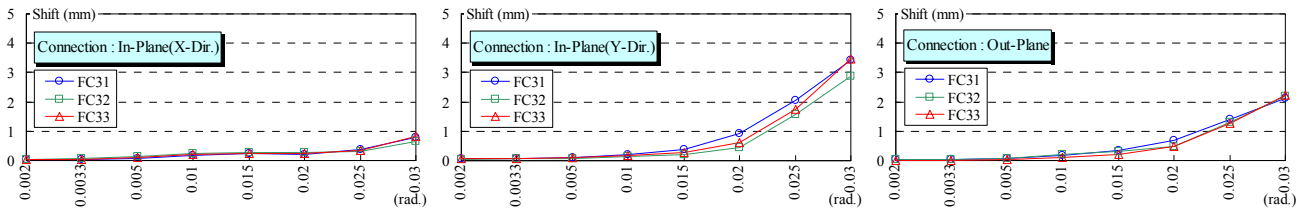


Figure 7 Shift of the beam-column connection

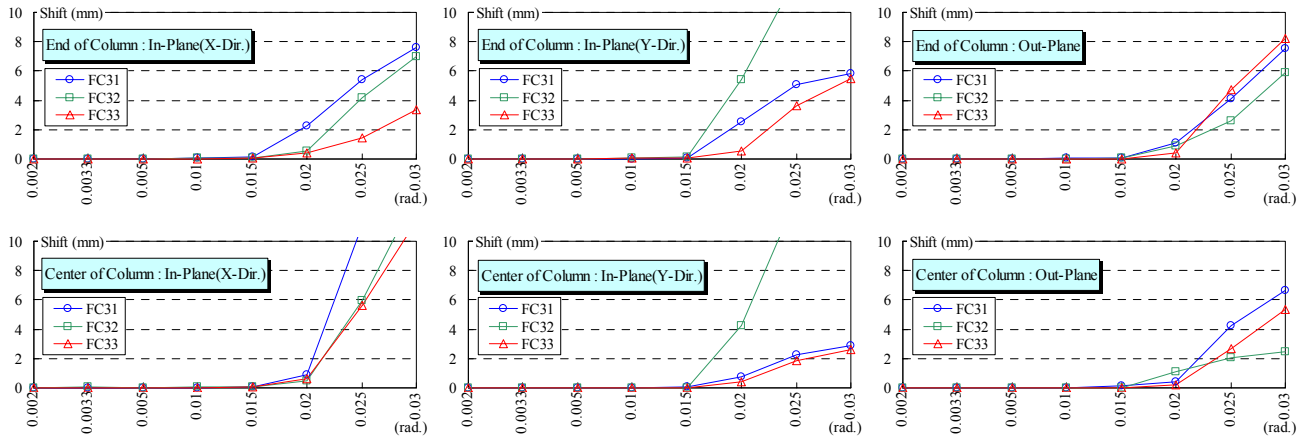


Figure 8 Shift of the boundary of columns

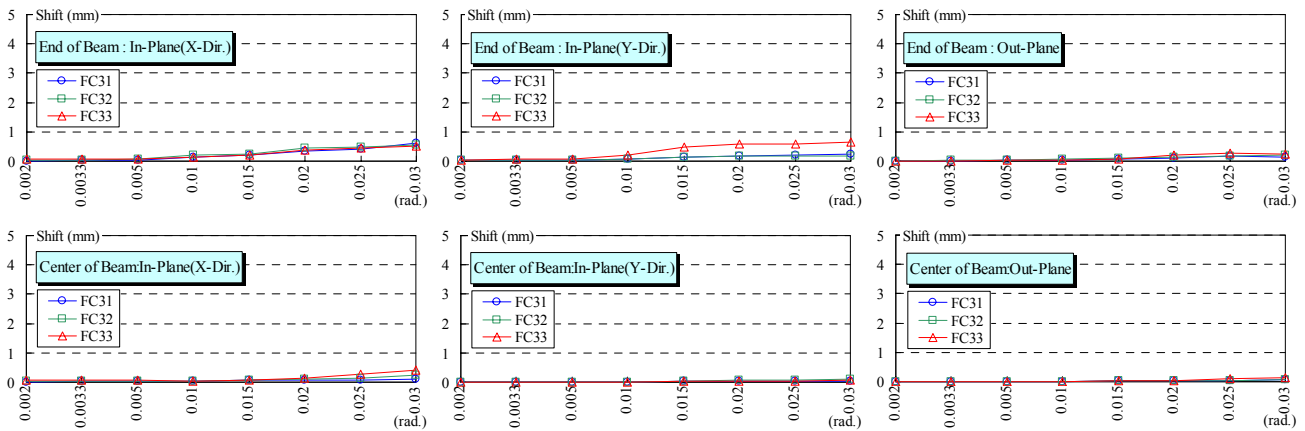


Figure 9 Shift of the boundary of beams

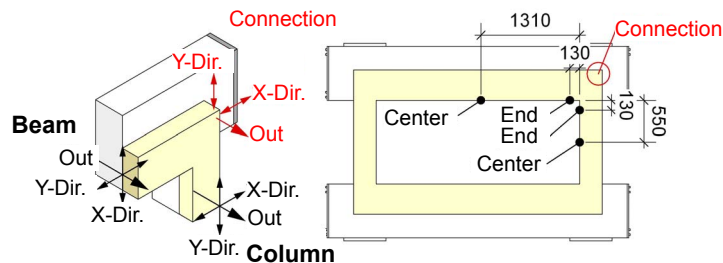


Figure 10 Definition in direction of each shearing and the measurement locations